Device research on GaAs-based InAlAs/InGaAs metamorphic high electron mobility transistors grown by metal organic chemical vapour deposition*

Xu Jing-Bo(徐静波)†, Zhang Hai-Ying(张海英), Fu Xiao-Jun(付晓君), Guo Tian-Yi(郭天义), and Huang Jie(黄 杰)

Institute of Microelectronics, Chinese Academy of Sciences, Beijing 100029, *China*

(Received 25 May 2009; revised manuscript received 9 June 2009)

This paper applies a novel quad-layer resist and e-beam lithography technique to fabricate a GaAs-based InAlAs/InGaAs metamorphic high electron mobility transistor (HEMT) grown by metal organic chemical vapour deposition (MOCVD). The gate length of the metamorphic HEMT was 150 nm, the maximum current density was 330 mA/mm, the maximum transconductance was 470 mS/mm, the threshold voltage was −0.6 V, and the maximum current gain cut-off frequency and maximum oscillation frequency were 102 GHz and 450 GHz, respectively. This is the first report on tri-termination devices whose frequency value is above 400 GHz in China. The excellent frequency performances promise the possibility of metamorphic HEMTs grown by MOCVD for millimetre-wave applications, and more outstanding device performances would be obtained after optimizing the material structure, the elaborate T-gate and other device processes further.

Keywords: GaAs-based metamorphic HEMT, maximum current gain cut-off frequency, maximum oscillation frequency, T-gate

PACC: 7340L, 7280E

1. Introduction

III-V compound semiconductor devices, such as GaAs- and InP-base high electron mobility transistors (HEMTs) and heterojunction bipolar transistors (HBTs),[1,2] are considered promising candidates for high-speed circuits. Especially, HEMTs are attractive devices for microwave/millimetre-wave low-noise, high-gain applications. The In content of InP-based HEMTs can reach 53% and provide higher mobility and two dimensional electron gas (2DEG) density than those of GaAs-based pseudomorphic HEMTs (PHEMT)s;[3,4] thus, the performances of InP-based HEMTs are superior to those of GaAs-based PHEMTs. The maximum current gain cutoff frequency (f_{T}) and maximum oscillation frequency ($f_{\max}$) are as high as 385 GHz and 1.1 THz for InP HEMTs with a sub 50nm T-gate respectively.[5] However, the disadvantages of InP HEMTs, low yield and high cost, are severe limits for applications, since the InP substrates are fragile, and wafer size is small.

To overcome these problems, GaAs-based metamorphic HEMTs (MHEMTs) have been the focus of many researchers,[6−11] as MHEMTs have InAlAs/InGaAs epitaxial layers on a GaAs substrate, so that they have the potential ability to combine the outstanding device performances of InP-based HEMTs with the advantages of economies of scale and robustness offered by conventional GaAs processing. Recently, with the development of the epitaxial growth technique, the quality of the active layers of MHEMTs has been improved, and then the MHEMTs, which are comparable to InP-based HEMTs, have been reported.[12−14] As far as we know, there are few reports on MHEMT devices grown by metal organic chemical vapour deposition (MOCVD), but many reports on MHEMT devices grown by molecular beam epitaxy (MBE). We have reported 200 nm T-gate MHEMTs grown by MBE with 105 GHz f_{T} and 70 GHz $f_{\max}$ by a tri-layer resist structure and the electron beam lithography technique.[15]

In this paper, a novel quad-layer resist and e-beam lithography technology was applied to develop the T-gate fabrication process, and developed 150 nm gate length MHEMTs grown by MOCVD with 102 GHz f_{T} and 450 GHz $f_{\max}$ simultaneously. The results demonstrate the excellent high frequency char-

*Project supported by the State Key Development Program for Basic Research of China (Grant No. G2002CB311901) and Institute of Microelectronics, Chinese Academy of Sciences, Dean Fund (Grant No. 06SB124004).

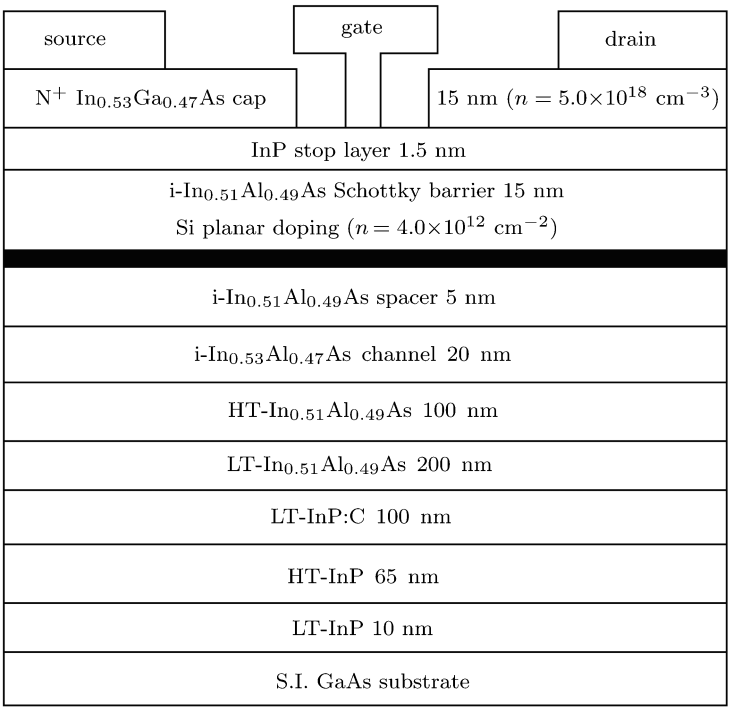
†Corresponding author. E-mail: xujingbo@ime.ac.cn

© 2010 Chinese Physical Society and IOP Publishing Ltd

acteristics of the MHEMT devices, noticeablely, the outstanding f_{max} performance is beneficial to W-band applications.

2. Device fabrication

MHEMT epitaxial wafers were grown on semi-insulting GaAs substrates by MOCVD technology. Figure 1 shows the layer structure of InAlAs/InGaAs MHEMT. The structure consists of multiple buffer layers (a 10 nm low temperature InP layer, a 65 nm high temperature InP layer, a 100 nm low temperature InP:C layer, a 200 nm low temperature $In_{0.51}Al_{0.49}As$ layer, a 100 nm high temperature $In_{0.51}Al_{0.49}As$ layer), a 20 nm $In_{0.53}Ga_{0.47}As$ channel, a 5 nm $In_{0.51}Al_{0.49}As$ spacer, a planar doping layer (Si: $4.0\times10^{12}cm^{-2}$), a 15 nm $In_{0.51}Al_{0.49}As$ Schottky barrier layer, a 1.5 nm InP etching stop layer and a 15 nm $N^{+}In_{0.53}Ga_{0.47}As$ cap layer (Si: 5.0×10^{18} cm^{-3}).



(a)

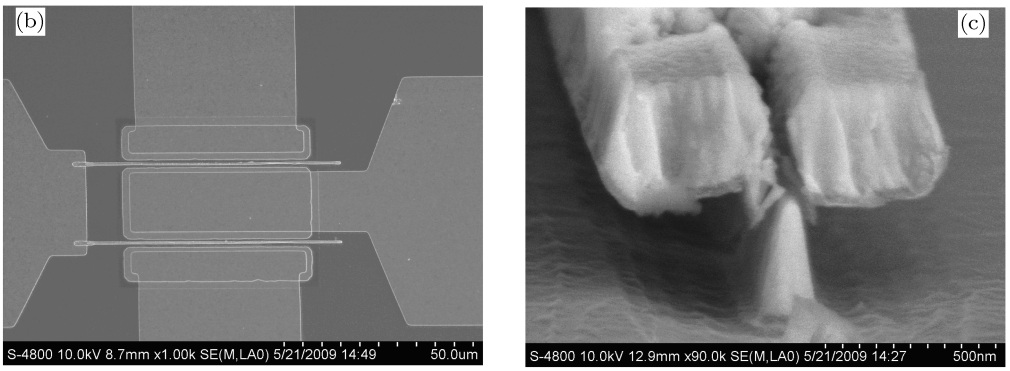


Fig. 1. MHEMT material and device structure, device planar picture and T-gate SEM photo. (a) MHEMT material and device structure; (b) SEM photo of the MHEMT device, the gate width is 50×2 μm; (c) SEM photo of the T-gate, the lengths of the gate foot and head are 150 nm, 1000 nm, respectively.

The metals of source and drain electrodes were formed by sequential evaporation of Ni/Ge/Au/Ge/Ni/Au (4:4:66:8:3:250 nm), and a contact resistance of 1.3×10^{-5} $\Omega\cdot$cm^2 was obtained after an alloy process at 280 °C for 10 min. The mesa isolation process was carried out by sequentially etching the cap layer using a phosphoric acid-based (H_3PO_4: H_2O_2 : H_2O=3:1:50) solution, etching the InP layer using a HCl-based (HCl:H_2O=1:1) solution, and etching other active layers ($In_{0.51}Al_{0.49}$ and $In_{0.53}Ga_{0.47}As$) also by using a phosphoric acid-based solution.

A quad-layer (PMGI/ZEP 520A/PMGI/PMMA) resist structure was used to pattern the T-shape resist profile. A poly-dimethyl gutarinide (PMGI) resist was used as a bottom layer, ZEP as a second layer, PMGI as a third layer, and PMMA as a top layer. The use of the bottom PMGI resist is helpful to remove the ZEP resist. One lithography step was employed, the gate recess area was exposed at 500 μC/cm^2. The top poly-methyl methacrylate (PMMA) layer was selectively developed in methylisobutylketone (MIBK)/isopropanol (IPA) (3 : 1) for 9 min. The next PMGI layer was selectively developed in TAHM/H_2O (1:4) developer for 50 s. Now, only the head of the T-gate was developed; the ZEP and bottom PMGI layer remain. The ZEP layer was selectively developed in ZEP-N50 for 60 s. Finally, the bottom PMGI layer was also developed in TAHM/H_2O (1:4) for 20 s. Gate recessing was performed by using citric-acid-based (citric acid: H_2O_2=1:1) solution, then evaporated Ti/Pt/Au (25:25:300 nm) gate metal. After a standard lift off process, the 150 nm T-gate was successfully fabricated and the width of the gate head was 1000 nm. Compared with MHEMT devices which we have reported previously,[15] the 150 nm T-gate process was advanced, and the wide gate head will also enhance device performances. It was beneficial to achieve excellent MHEMT devices and circuits for millimetre-wave applications. A scanning electron microscope (SEM) photo of the 150 nm T-gate is shown in Fig. 1(c).

3. Results and discussion

The direct current (DC) characteristics of the MHEMTs were measured by a HP 4155 semiconductor parameter analyser. The transfer and transconductance curves are shown in Fig. 2(a). The peak transconductance G_m is 470 mS/mm, when V_{ds} = 2.0 V and V_{gs} = −0.2 V. The pinch-off voltage is −0.6 V derived from the transfer curves. The $I_{ds}-V_{ds}$ curves are shown in Fig. 2(b).

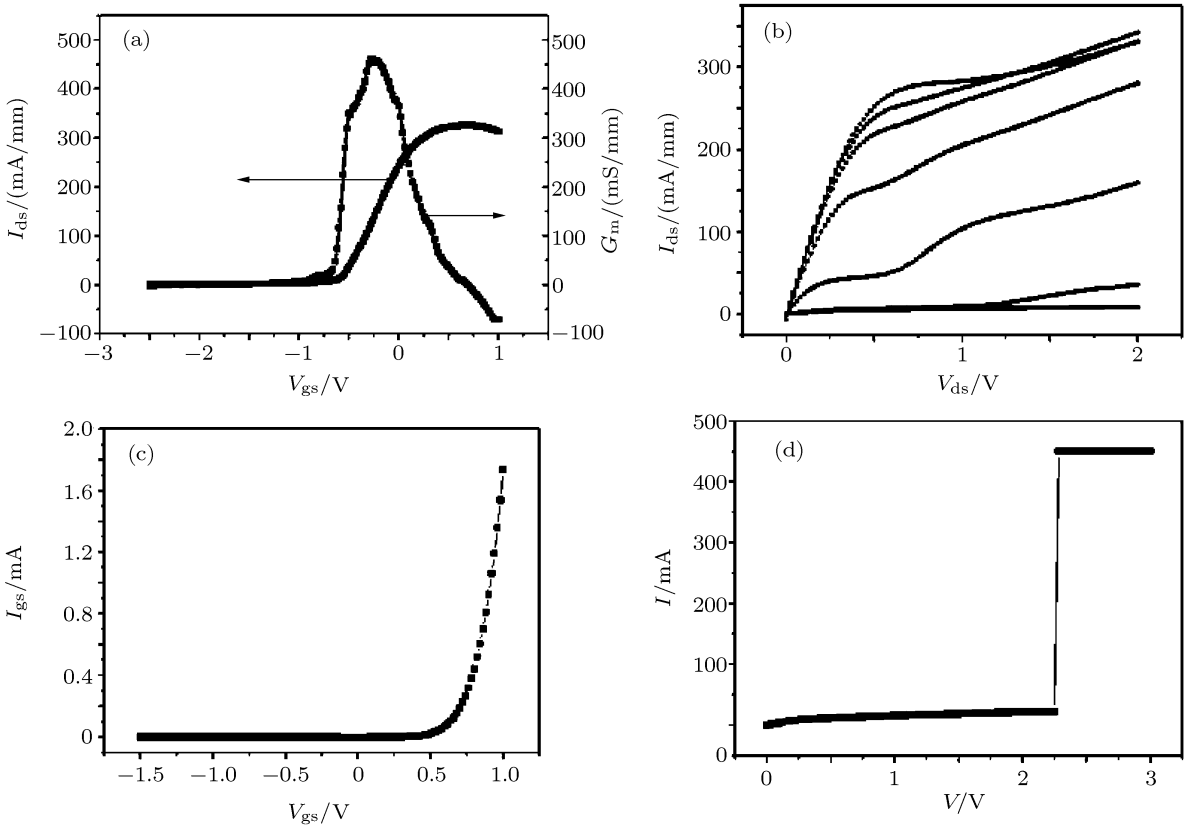


Fig. 2. DC performances of the MHEMT device. (a) Transfer and transconductance curves; (b) $I_{ds} - V_{ds}$ curves; (c) $I_{gs} - V_{gs}$ curve; (d) on-state breakdown characteristic (V_{ds} = 0.0 V).

The maximum current density is 330 mA/mm, while V_{ds} ranges from 0.0 V to 2.0 V, V_{gs} changes from −0.8 V to 1.0 V, and the step is 0.3 V. The $I_{gs}-V_{gs}$ curve is shown in Fig. 2(c). The Schottky barrier height, defined as the gate–source voltage when the gate–source current is 0.1 mA, is about 0.65 V. The on-state (V_{ds} = 0.0 V) breakdown characteristic is shown in Fig. 2(d). The on-state (V_{ds} = 0.0 V) breakdown voltage is 2.25 V. If the MHEMT material structure would be optimized by appropriately increasing the doping doses of the planar layer and the cap layer, the DC performances could be improved further.

The radio frequency (RF) characteristics were obtained through on-wafer S-parameter measurements at frequencies up to 26.1 GHz increasing in 0.1 GHz increments by using an HP 8510C vector network analyser and on-wafer probes. Figure 3 shows the frequency dependence of current gain $|H_{21}|^2$, maximum available gain (MAG)/maximum stable gain (MSG) and unilateral power gain (U) of the 150 nm T-gate MHEMT under a drain–source voltage of 2.0 V and a gate–source voltage of −0.2 V. The f_T is 102 GHz by extrapolating the current gain curve to the −20 dB/decade line. After extracting parasitical parameters and a de-embeding process, the different f_{max} values are derived from MAG/MSG and the U method. Because the slope of MAG/MSG is −10 dB/decade, not −20 dB/decade yet, at the extrapolating dot, the f_{max} of 200 GHz from the MAG/MSG curve is lower than the real value. Since the slope of the unilateral power gain curve is −20 dB/decade, the f_{max} of 450 GHz derived from the U curve is more reliable than that derived from the MAG/MSG curve.

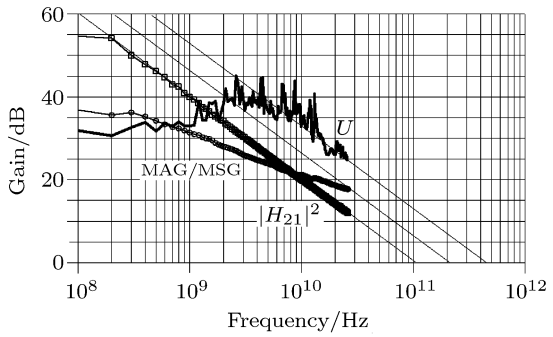


Fig. 3. RF performances of the fabricated 150 nm T-gate MHEMT. At the gate bias V_{gs} = −0.2 V and the drain bias V_{ds} = 2.0 V, the device shows f_T of 102 GHz (circle+line) and f_{max} of 200 GHz derived from the MAG/MSG curve (square+line) or f_{max} of 450 GHz derived from the U curve (line).

As far as we know, this is the first report on tri-termination devices whose frequency value is above 400 GHz in China. The excellent frequency performances promise the possibility of millimetre-wave applications, especially for W-band millimetre-wave devices and circuits. More outstanding device performances would be obtained after optimizing the material structure, the elaborate T-gate and other device processes further.

4. Conclusion

In summary, we have fabricated 150 nm gate length InAlAs/InGaAs MHEMTs with a quad-layer resist structure. The devices showed good DC characteristics, and the peak transconductance, maximum current density and pinch-off voltage were 470 mS/mm, 330 mA/mm and −0.6 V, respectively. Excellent RF characteristics were obtained. The f_T is 102 GHz, and f_{max} is 450 GHz. We found that the ultrahigh f_{max} value was a result of the elaborate T-gate process; the outstanding f_{max} performance of MHEMT devices promises the possibility of millimetre-wave applications. The DC and RF characteristics would be improved further after optimization of material structure, T-gate and other device fabrication processes.

Acknowledgement

The authors would like to thank the Department of Electronic and Computer Engineering, Hong Kong University of Science and Technology for providing the GaAs-based MHEMT material grown by MOCVD. The authors would also like to thank Li Yan-Kui for the help with the RF measurement. Finally, the authors would like to thank Dr. Li Hai-Ou and Dr. Cheng Wei for fruitful discussions.

References

[1] Jin Z, Su Y B, Cheng W, Liu X Y, Xu A H and Qi M 2008 *Chin. Phys. Lett.* **25** 2686

[2] Zhou S L, Huang H, Huang Y Q and Ren X M 2007 *Acta Phys. Sin.* **56** 2890 (in Chinese)

[3] Li D L and Zeng Y P 2006 *Chin. Phys.* **15** 2735

[4] Yoshimi Y, Akira E, Keisuke S, Kohki H, Toshiaki M,

Satoshi H and Takashi M 2002 *IEEE Electron Device Letter* **23** 573

[5] Lai R, Mei X B, Deal W R, Yoshida W, Kim Y M, Liu P H, Lee J, Uyeda J, Radisic V, Lange M, Gaier T, Samoska L and Fung A 2007 *IEEE International Electron Devices Meeting* 10–12 2007 Washington p609

[6] Qiu Z J, Jiang C P, Gui Y S, Shu X Z, Guo S L, Chu J H, Cui L J, Zeng Y P, Zhu Z P and Wang B Q 2003 *Acta Phys. Sin.* **52** 2879 (in Chinese)

[7] Li H O, Tang C W and Lau K M 2008 *IEEE Electron Device Letters* **29** 561

[8] Maher H, Makoudi I E, Frijlink P, Smith D, Rocchi M, Bollaert S, Lepilliet S and Dambrine G 2007 *IEEE Trans. on Electron Devices* **54** 1626

[9] Lee K W, Lee K L, Lin X Z, Tu C H and Wang Y H 2007 *IEEE Trans. on Electron Devices* **54** 418

[10] Lin C K, Wang W K, Chan Y J and Chiou H K 2005 *IEEE Trans. on Electron Devices* **52** 1

[11] Hsu W C, Chen Y J, Lee C S, Wang T B, Huang J C, Huang D H, Su K H, Lin Y S and Wu C L 2005 *IEEE Trans. on Electron Devices* **52** 1079

[12] Lee K S, Kim Y S, Hong Y K and Jeong Y H 2007 *IEEE Electron Device Letters* **28** 672

[13] Lim B O, Lee M K, Baek T J, Han M, Kim S C and Rhee J K 2007 *IEEE Electron Device Letters* **28** 546

[14] Elgaid K, McLelland H, Holland M, Moran D A J, Stanley C R and Thayne I G 2005 *IEEE Electron Device Letters* **26** 784

[15] Xu J B, Zhang H Y, Fu X J, Guo T Y and Huang J 2008 *Chin. Sci. Bullet.* **53** 3585